Review of the contact pressure model for evaluation of the penetration tube ejection from a reactor lower head during a severe accident

Kukhee Lim*, Yong Jin Cho, Yoonhee Lee, and Jin-Seong Park
Korea Institute of Nuclear Safety
62 Gwahak-ro, Yuseong-gu, Daejeon, Korea 34142
** Corresponding author: limkh@kins.re.kr*

1. Introduction

When damaged core materials are relocated to the reactor lower head with penetrations during a severe accident, the loss integrity of the reactor pressure vessel caused by this type of penetration failure will occur earlier than the global failure of the reactor lower head. Tube ejection out of the reactor lower head is the representative penetration tube failure models suggested by NUREG/CR-5642 [1]. When the penetration tube is locked at the contact interface between the tube and the reactor lower head by interference, the frictional shear force at the interface, which is determined by the contact pressure, should be evaluated in order to assess the tube ejection failure. In this study, the previous contact pressure model [1] is reviewed and the model is improved by considering the deformation of the reactor lower head.

2. Review of the previous model

The applied force to reactor lower head and the interface between penetration tube and hole in the reactor lower head by RCS internal pressure is shown in Fig. 1. The ejection of a penetration tube can be resisted by high friction force at the interface of tube and hole. If the weld is failed and the friction force defined by Eq. 1 is less than ejection force by internal pressure, the tube will be ejected.

$$F_f = \int dF_f = \int_0^{l_f} f \cdot P_s \cdot 2\pi r_o \cdot dl \qquad (1)$$

where F_f : friction force,
f : friction coefficient at the interface,
l_f : length of contact interface,
P_s : contact pressure,
r_o : outer radius of tube.

The contact pressure between tube and penetration hole P_s is evaluated by Eqs. 2 and 3.

$$\delta < 0,\ \ P_s = lesser\ of \begin{cases} \frac{\delta \cdot E\left(r_o^2 - r_i^2\right)}{r_o[r_o^2(1-2\nu_t)+r_i^2(1+\nu_t)} \\ \frac{2}{\sqrt{3}}\sigma_u \ln\left(\frac{r_o}{r_i}\right) \end{cases} \qquad (2)$$

$$\delta \geq 0,\ \ P_s = 0 \qquad (3)$$

where δ: difference of displacement between tube and hole.

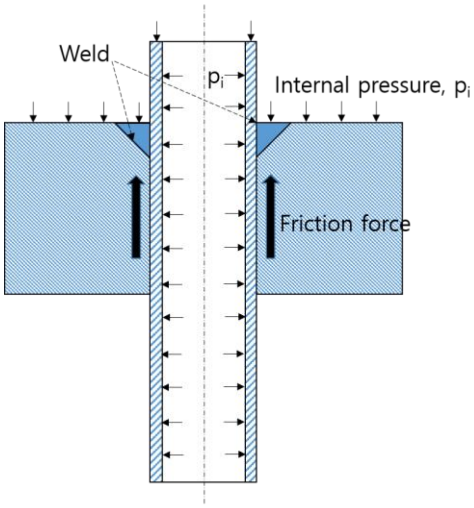

Fig. 1. Schematic of a mechanical load at a penetration area

3. Derivation of the contact pressure

For a single hollow cylinder describing a penetration tube, force equilibrium equation of a volume element can be expressed as Eq. 4.

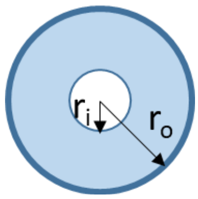

Fig. 2. Cross-section of one hollow tube

$$\frac{\sigma_r - \sigma_\theta}{r} + \frac{d\sigma_r}{dr} = 0 \qquad (4)$$

where σ_r and σ_θ: radial and circumferential stress.

For a hollow cylinder whose inner radius is r_a and outer radius is r_b , the following boundary conditions of $\sigma_r(r_a) = P_a$ and $u(r_b) = u_b$ are applied. Then, σ_r becomes

$$\sigma_r = \frac{E}{(1+\nu)r_a^2+(1-\nu-2\nu m)r_b^2}\left\{u_b r_b\left(1-\frac{r_a^2}{r^2}\right)+\frac{P_a r_a^2}{E}\left[(1+\nu)+(1-\nu-2\nu m)\frac{r_b^2}{r^2}\right]\right\} \qquad (5)$$

The pressure at the outer surface P_b, which is σ_r in Eq. 24 at $r = r_b$, becomes

$$P_b = \frac{E}{(1+\nu)r_a^2+(1-\nu-2\nu m)r_b^2}\left[u_b r_b\left(1-\frac{r_a^2}{r_b^2}\right)+\frac{2(1-\nu m)P_a r_a^2}{E}\right] \quad (6)$$

If P_a is negligibly small and $m=\frac{1}{2}$, Eq. 6 becomes

$$P_b = \frac{E u_b(r_b^2-r_a^2)}{r_b[(1+\nu)r_a^2+(1-\nu)r_b^2]} \quad (7)$$

The contact pressure of NUREG/CR-5642 in the elastic region equals Eq. 7 when $u_b=\delta$, $r_a=r_i$ and $r_b=r_o$.

If the material behaves perfectly plastic, the following maximum and minimum principal stress can be considered for a hollow cylinder.

- Case 1: σ_θ and σ_r are maximum and minimum stresses.
- Case 2: σ_θ and σ_z are maximum and minimum stresses.

where σ_r, σ_θ, and σ_z are radial, hoop and axial stress, respectively.

For the plane strain or free-closed ends conditions, it satisfies the Tresca yield criterion. Especially for the free-closed ends condition, it satisfies the von Mises yield criterion, too [2]. Generally, the relationship between the maximum and minimum principal stress is expressed by this equation.

$$\sigma_\theta - \sigma_r = k\sigma_Y \quad (8)$$

where $k=1$ (for the Tresca yield criterion)
$k=\frac{2}{\sqrt{3}}$ (for the von Mises yield criterion)
σ_Y: yield strength

For Case 2, it only satisfies the following Tresca yield criterion.

$$\sigma_\theta - \sigma_z = \sigma_Y \quad (9)$$

Because $\sigma_z = 0$ for the plane stress condition, Eq. 3 becomes

$$\sigma_\theta = \sigma_Y \quad (10)$$

By assuming the radial and hoop stress as σ_{re} and $\sigma_{\theta e}$ in the elastic region, and σ_{rp} and $\sigma_{\theta p}$ as in the plastic region, the analytical solution for the each stress component can be derived as follows:

(For Case 1):
By substituting Eq. 2 into the equilibrium equation and using integration, σ_{rp} is expressed by Eq. 5.

$$\frac{\sigma_{rp}-\sigma_{\theta p}}{r}+\frac{d\sigma_{rp}}{dr}=0$$
$$\rightarrow \sigma_{rp} = k\sigma_Y \ln r + C_1 \quad (11)$$

where r and C_1 are radius and the integral constant.

$\sigma_{\theta e}$ and σ_{re} are expressed in Eqs. 12 – 13 by the analytical solution of the equilibrium equation about the radial displacement u in the elastic region.

$$\sigma_{re} = \frac{E}{(1+\nu)(1-\nu-2\nu m)}\left[(1+\nu)C_2-(1-\nu-2\nu m)\frac{1}{r^2}C_3\right] \quad (12)$$
$$\sigma_{\theta e} = \frac{E}{(1+\nu)(1-\nu-2\nu m)}\left[(1+\nu)C_2+(1-\nu-2\nu m)\frac{1}{r^2}C_3\right] \quad (13)$$

where E, ν, and m are the elastic modulus, Poisson's ratio, and indicator for the stress and strain condition (ν, 0 and $\frac{1}{2}$ for the plane strain, plain stress and free-closed ends, respectively).

The radial displacement u in the plastic region is expressed in Eq. 14.

$$u = C_4 r + C_5\frac{1}{r} \quad (14)$$

where C_4 and C_5 are the integral constants.

By applying the internal pressure P_a and displacement u_b at the external surface for a hollow cylinder with the inner and outer radius r_a and r_b, respectively, the boundary conditions which yield starts at $r=r^*$ are as follows:

$$\begin{aligned} &r=r_a,\ \sigma_{rp}=P_a\\ &r=r_b,\ u=u_b\\ &r=r^*,\ \sigma_{\theta e}-\sigma_{re}=k\sigma_Y\\ &r=r^*,\ \sigma_{re}=\sigma_{rp} \end{aligned} \quad (15)$$

According to Eqs. 11 – 14, P_a, P_b and u_b become

$$u_b = \frac{(1-\nu-2\nu m)r_b}{E}\left(k\sigma_Y \ln\frac{r^*}{r_a}+P_a\right)+\frac{k\sigma_Y r_b}{2E}\left[(1+\nu)\frac{r^{*2}}{r_b^2}+(1-\nu-2\nu m)\right] \quad (16)$$

Therefore, σ_{re}, $\sigma_{\theta e}$, σ_{rp}, and $\sigma_{\theta p}$ becomes

$$\sigma_{re} = \frac{E}{(1-\nu-2\nu m)}\left\{\frac{u_b}{r_b}-\frac{k\sigma_Y r^{*2}}{2E}\left[\frac{(1+\nu)}{r_b^2}+\frac{(1-\nu-2\nu m)}{r^2}\right]\right\} \quad (17)$$
$$\sigma_{\theta e} = \frac{E}{(1-\nu-2\nu m)}\left\{\frac{u_b}{r_b}-\frac{k\sigma_Y r^{*2}}{2E}\left[\frac{(1+\nu)}{r_b^2}-\frac{(1-\nu-2\nu m)}{r^2}\right]\right\} \quad (18)$$
$$\sigma_{rp} = k\sigma_Y \ln\frac{r}{r_a}+P_a \quad (19)$$
$$\sigma_{\theta p} = k\sigma_Y\left(\ln\frac{r}{r_a}+1\right)+P_a \quad (20)$$

By using Eqs. 17 and 19, the external pressure P_b at $r = r_b$ for a cylinder at the partially plastic state and fully plastic state is given by the following relation.

(Partially plastic state, $r_a \le r^* \le r_b$):

$$P_b = \sigma_{re}(r_b) = \frac{E}{(1-\nu-2\nu m)}\left[\frac{u_b}{r_b} - \frac{(1-\nu m)k\sigma_Y}{E}\frac{r^{*2}}{r_b^2}\right] \quad (21)$$

(Fully plastic state, $r^* = r_b$):

$$P_b = \sigma_{rp}(r_b) = k\sigma_Y \ln\frac{r}{r_a} + P_a \quad (22)$$

(For Case 2):
By substituting Eq. 10 into the equilibrium equation and using integration, σ_{rp} is expressed by Eq. 23.

$$\frac{\sigma_{rp}-\sigma_{\theta p}}{r} + \frac{d\sigma_{rp}}{dr} = 0$$
$$\rightarrow \sigma_{rp} = \sigma_Y + \frac{C_1}{r} \quad (23)$$

σ_{re}, $\sigma_{\theta e}$ and u are obtained by substituting $m = 0$ into Eqs. 6 – 8. The boundary conditions are same with the Case 1 except $\sigma_{\theta e}$ at $r = r^*$. The changed boundary condition is given in Eq. 23.

$$r = r^*, \quad \sigma_{\theta e} = \sigma_Y \quad (24)$$

By applying boundary conditions into Eq. 14, u_b becomes

$$u_b = \frac{r_b}{E}\left[(1-\nu)\left(1-\frac{r_a}{2r^*}\right) + \frac{(1+\nu)r^* r_a}{2r_b^2}\right]\sigma_Y + \frac{r_a r_b}{2E}\left[\frac{(1-\nu)}{r^*} - \frac{(1+\nu)r^*}{r_b^2}\right]P_a \quad (25)$$

Therefore, σ_{re}, $\sigma_{\theta e}$, σ_{rp}, and $\sigma_{\theta p}$ becomes

$$\sigma_{re} = \frac{E}{(1-\nu)}\left\{\frac{u_b}{r_b} - \frac{r^* r_a(\sigma_Y - P_a)}{2E}\left[\frac{(1+\nu)}{r_b^2} + \frac{(1-\nu)}{r^2}\right]\right\} \quad (26)$$
$$\sigma_{\theta e} = \frac{E}{(1-\nu)}\left\{\frac{u_b}{r_b} - \frac{r^* r_a(\sigma_Y - P_a)}{2E}\left[\frac{(1+\nu)}{r_b^2} - \frac{(1-\nu)}{r^2}\right]\right\} \quad (27)$$
$$\sigma_{rp} = \left(1-\frac{r_a}{r}\right)\sigma_Y + \frac{r_a}{r}P_a \quad (28)$$
$$\sigma_{\theta p} = \sigma_Y \quad (29)$$

By using Eqs. 26 and 28, the external pressure P_b at $r = r_b$ for a cylinder at the partially plastic state and fully plastic state is given by the following relation.

(Partially plastic state, $r_a \le r^* \le r_b$):

$$P_b = \frac{E}{(1-\nu)}\left[\frac{u_b}{r_b} - \frac{r^* r_a(\sigma_Y - P_a)}{E r_b^2}\right] \quad (30)$$

(Fully plastic state, $r^* = r_b$):

$$P_b = \sigma_Y - \frac{r_a}{r_b}(\sigma_Y - P_a) \quad (31)$$

If P_b corresponds to P_s in the lower part of Eq. 2, P_b is identical to P_s in the lower part of Eq. 2 at $k = \frac{2}{\sqrt{3}}$, $\sigma_y = \sigma_u$, $r_a = r_i$, $r_b = r_o$ and $P_a = 0$. Therefore, the assumptions of the previous contact pressure relation in NUREG/CR-5642 can be summarized as follows:

- Assumption 1: negligible internal pressure ($P_a = 0$)
- Assumption 2: free-closed ends ($\sigma_z = \frac{1}{2}(\sigma_r + \sigma_\theta)$)
- Assumption 3: one hollow cylinder configuration
- Assumption 4: a cylinder in fully plastic state
- Assumption 5: application of the von Mises yield criterion ($k = \frac{2}{\sqrt{3}}$)
- Assumption 6: evaluation of pressure at rupture by using σ_u instead of σ_Y

4. Validation

Two-dimensional axisymmetric finite element models of the ICI penetration tube using ANSYS Mechanical R18.0 are constructed in order to validate the derived assumptions of the contact pressure model. PLANE183, an 8-node element with mid-nodes, is selected for meshing. Half of the ICI penetration tube in the length direction is modeled using a symmetry condition. The geometry according to the stress and strain conditions with the dimension in Table 1 are shown in Fig. 3. In the free-closed ends condition shown in Fig. 3, a physical cap part at the upper surface of the axisymmetric tube is considered, and its outer surface is loaded by pressure corresponding to the contact pressure by δ . The geometrical nonlinearity is not considered because the derived equations in Chap. 3 assumes no changes of the geometrical domain. The σ_r according to r and δ at 400 K with the free-closed end condition is shown in Fig. 4 – 7. The σ_r with von Mises yield criterion by Eqs. 17 and 19 follows the FEM result very well

Table 1. Geometry of the ICI penetration tube for finite element modeling

Inner radius (r_a)	9.5 mm
Outer radius (r_b)	38.1 mm
Length	175 mm

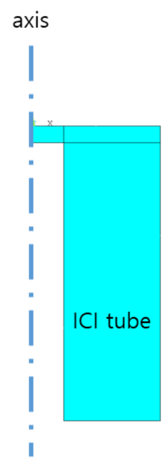

Fig. 3. Axisymmetric geometry according to the stress and strain conditions (one hollow cylinder)

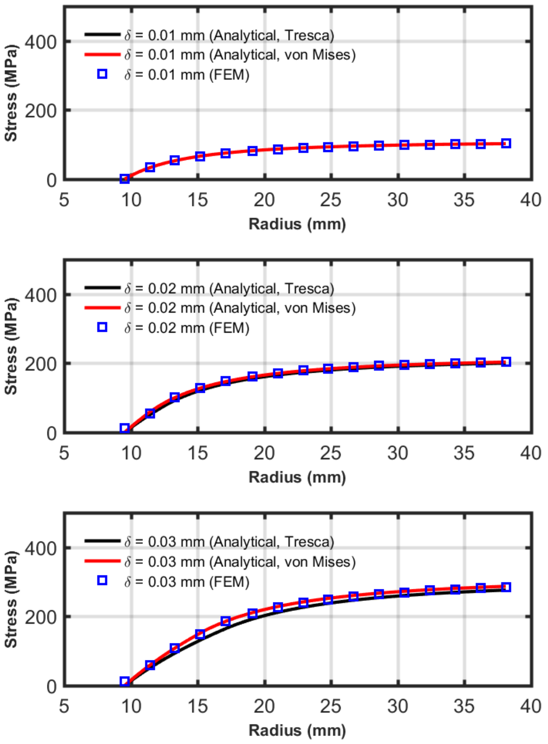

Fig. 4. σ_r according to r at 400 K with the free-closed end condition and δ = (0.01 – 0.03) mm

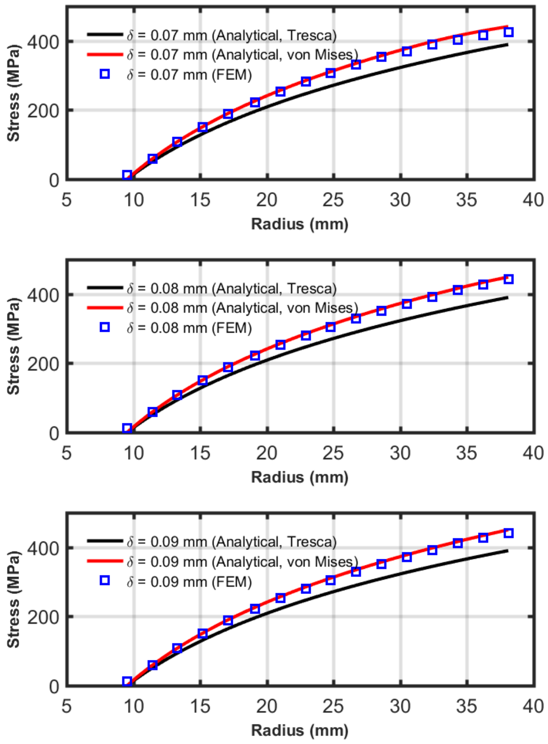

Fig. 6. σ_r according to r at 400 K with the free-closed end condition and δ = (0.07 – 0.09) mm

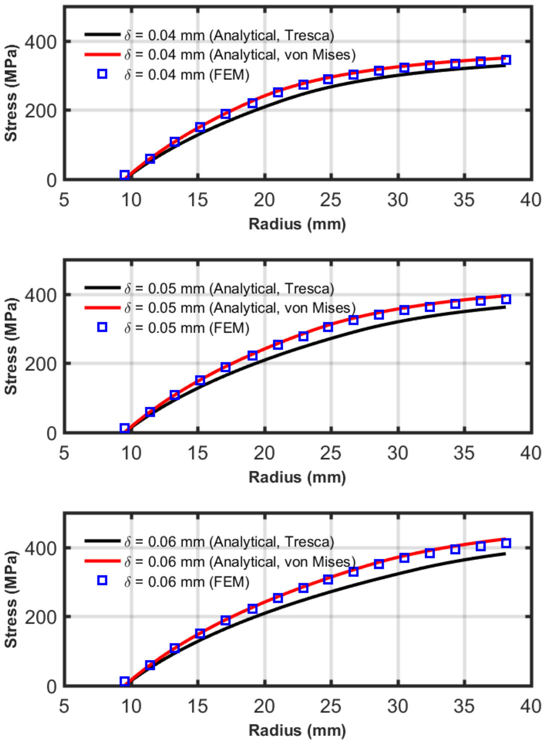

Fig. 5. σ_r according to r at 400 K with the free-closed end condition and δ = (0.04 – 0.06) mm

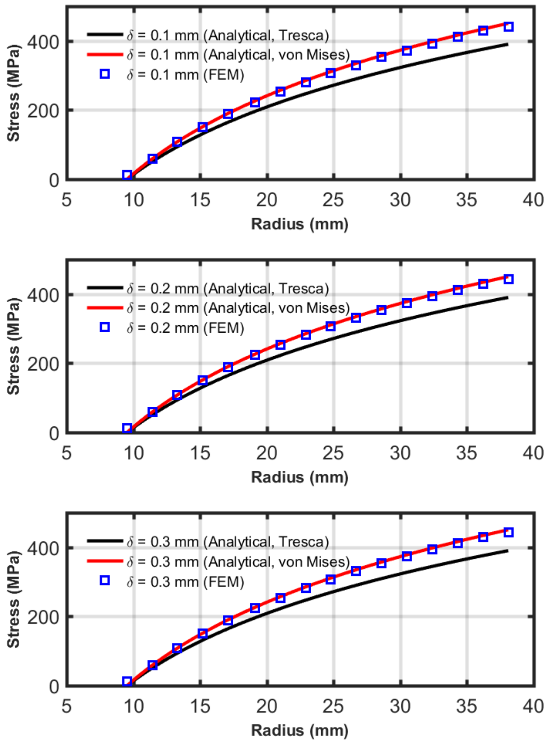

Fig. 7. σ_r according to r at 400 K with the free-closed end condition and δ = (0.1 – 0.3) mm

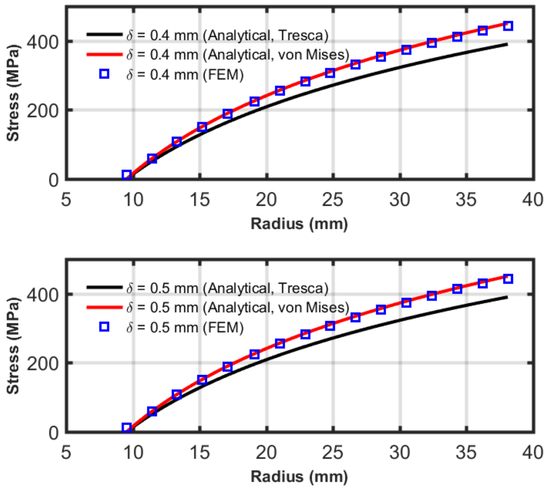

Fig. 8. σ_r according to r at 400 K with the free-closed end condition and $\delta = (0.4 – 0.5)$ mm

5. Conclusions

In this study, the contact pressure evaluation method from NUREG/CR-5642 has been reviewed. The assumptions of a geometrical configuration and the 'stress and strain condition' of the previous model in NUREG/CR-5642 are derived in a reversed manner by a stress analysis. As a result, it was found that the previous model only considers the deformation of the ICI penetration tube itself and it assumes the free-closed ends condition. However, these assumptions cannot explain the deformation of the reactor lower head hole. And more general stress and strain conditions are needed to explain the mounting condition of the penetration tube. And the previous model considers the rupture pressure by using the ultimate strength instead of the yield strength for the analytical stress analysis which results in overestimated contact pressure. These drawbacks can be modified by choosing the configuration of two concentric hollow cylinders which represent the ICI penetration tube and the reactor lower head with a generalized expression of the stress and strain conditions and by using the yield strength.

ACKNOWLEDGEMENT

This work was supported by the Nuclear Safety Research Program through the Korea Foundation Of Nuclear Safety(KoFONS) using the financial resource granted by the Nuclear Safety and Security Commission(NSSC) of the Republic of Korea. (No. 2106007)

REFERENCES

[1] J. L. Rempe et al., Light Water Reactor Lower Head Failure Analysis, NUREG/CR-5642, 1993.